Recent advances in fiber-to-PIC packaging technologies for scalable manufacturing

K. Gradkowski*[a], H.-C. Wang[b], D. S. Kumar[a], S. Collins[a], S. Butler[a], H.-Y. Hwang[a], W. Noell[b], K. Shortiss[c], J. Parra[c], G. Fiol[d], K.-O. Velthaus[d], P. O'Brien[a]

[a]Photonics Packaging and Systems Integration, Tyndall National Institute, Lee Maltings, T12R5CP, Cork, Ireland; [b]Focuslight Switzerland SA, Rouges-Terres 61, CH 2068 Hauterive, Switzerland; [c]ficonTEC Ireland, Tyndall National Institute, Lee Maltings, T12R5CP, Cork, Ireland; [d]Fraunhofer Heinrich Hertz Institute, Einsteinufer 37, 10587 Berlin, Germany

ABSTRACT

We present a photonic packaging paradigm where the light from an edge coupler of a photonic integrated circuit is turned normal to the surface using a specially-manufactured silicon micro-lens equipped with an etched turning prism. Due to expansion of the beam, the alignment tolerances of coupling to similarly-equipped fiber array are significantly relaxed making it compatible with the future surface-mounted pluggable solutions. We demonstrate sub-2 dB coupling efficiency at 1310 nm from a transceiver chip.

Keywords: Photonic Integrated Circuits, Photonic Packaging, Micro-Optics, Expanded Beam Connectors, Scalable Packaging

1. INTRODUCTION

Photonics is experiencing a revolutionary period of growth spurred by an enormous potential of utilizing light for the purpose of high-speed, high-bandwidth communications [1], sensing [2] and biomedical engineering [3]. Photonic integrated circuits, or PICs, play a crucial role in these advancements as optical equivalents of electronic integrated circuits that have revolutionized the technology of the latter half of last century. In many modern designs, the photonic and electronic components of the device operate in close proximity, in a so-called co-packaged optics design paradigm [4][5]. Because of this, the packages are becoming much more complicated, requiring a growing number of electrical and optical I/O connections – the former reaching hundreds (including RF connections), while the latter are still in the low tens of fibers per device. In the state-of-the-art, optical fibers (bundled into fiber arrays, or FA) are permanently attached to the PICs [6][7], which is a serious bottleneck for scalable manufacturing as the process is serial, package-by-package. As a result, the growth of photonics, additionally driven by advances in AI and the subsequent increase in demand for high bandwidth optical transceivers, is at risk of being throttled back by manufacturing capacity.

One of the methods of addressing the manufacturing gap is to parallelize the optical packaging process and make it compatible with legacy microelectronics packaging pipelines, which among other things, includes reflow. Within that paradigm, a key enabling technology is expansion of the mode between the fiber and the PIC using micro-optics to physically separate the two elements, making them independent parts of the packaging process. While typical tolerances of alignment of fiber to the PIC are of the order of several microns [8], mode expansion can increase that by an order of magnitude. Not only does this allow for easier assembly of optical interfaces by relaxing fabrication restrictions on key mechanical elements of the package [9], it also facilitates pluggable photonic packaging. This method was demonstrated in the grating coupler [10], as well as in edge-coupling regimes [9][11].

So far, the micro-optics within packages are still being assembled on the package-by-package manual basis, although there are already attempts towards automation of the process [12]. For truly scalable manufacturing though, it not only has to be automated, but ideally being executed on a wafer-scale. This is conducive towards selection of grating couplers as they are surface features, therefore allowing for relatively easy assembly of micro-optics using machine vision and e.g. micro-transfer printing [13]. Grating couplers however suffer in comparison with edge couplers in terms of coupling efficiency

* kamil.gradkowski@tyndall.ie

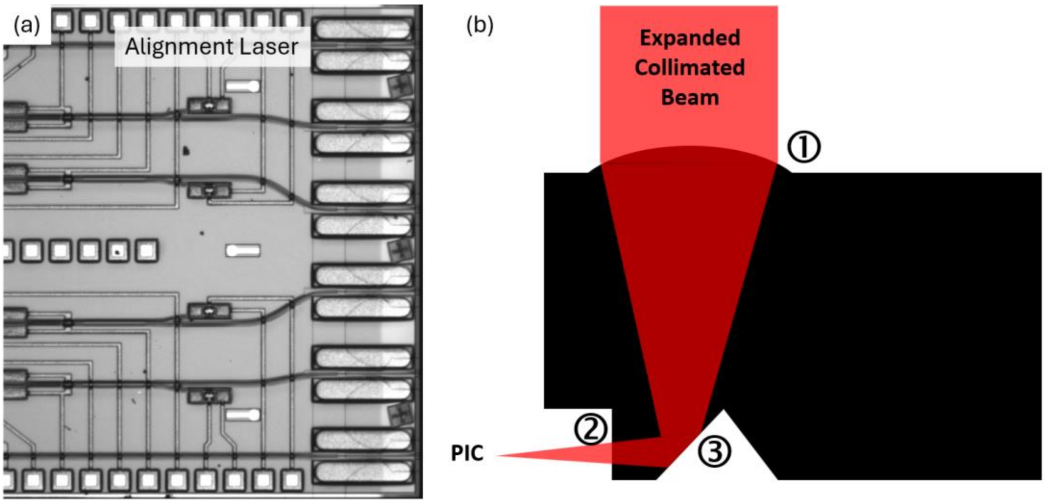

Figure 1. (a) Photograph of the coupler region of the PIC under investigation. (b) Schematic of the turning mirror lens. Numbered surfaces refer to different etching steps.

(CE), polarization sensitivity and bandwidth [14]. Therefore the optimal solution is to take advantage of edge couplers' superior performance and turn them into surface features for easy integration. This can be achieved by integration of a turning element into the body of a micro-lens to turn the light vertical.

This geometry holds a critical advantage over other implementations of the expanded beam connection scheme as it makes the alignment of the chip assembly easier. In other edge coupler examples [9][11] the chip stack has to be quite precisely assembled to match the height of the PIC with the respective connector socket counterpart. While the expansion of the beam makes this easier, it is not free from major sources of errors as the stack can be composed of several layers and include other elements, such as a heat spreader or a PCB. The manufacturing and assembly of all the individual parts carries fabrication and assembly tolerances, which can add up to a value beyond what the expanded beam connectors can provide (e.g. PICs themselves can have a 10μm thickness tolerance). Thus turning the light vertically eliminates the stack tolerance error and only relies on the relative positions of the PIC with respect to the socket, which can be aligned quite precisely using machine vision.

2. TURNING MIRROR LENS DESIGN AND FABRICATION

The work outlined below demonstrates an implementation of the idea of turning beam expanded connector for a datacoms transceiver PIC. The chip is based on the InP platform and contains 4 Tx channels along with an alignment channel to couple light to an optical fiber during packaging. The photograph of the coupler region of the PIC is presented in Figure 1(a). The measured mode-field diameter (MFD) of the edge coupler is asymmetrical: 3.7 μm in the x-direction (corresponding to the edge of the chip) and 2.9 μm in the y-(vertical)-direction. The operating wavelength is 1310 nm.

The schematic of the vertical coupling lens is shown in Figure 1(b). It is made from silicon and has three primary working surfaces. The curved surface (1) takes the expanding beam and collimates it to interface with the connector. It is fabricated using Reactive Ion Etching (RIE). Surface (2) is fabricated using Deep RIE (DRIE) method to create a smooth surface that minimizes scattering of light since the lenses are created on a large wafer from which they are singulated using a dicing saw. A secondary purpose of the surface is to position it at a precise point to conserve the total optical path length of light through the structure from the PIC facet to the lens top that collimates the beam. For a working distance in air (an air gap between surface (2) and the PIC facet) of 65 μm, the total path of light through the lens is 550 μm with the wafer thickness being 500 μm. The radius of curvature (ROC) of surface (1) is selected to expand the beam in the x-direction to 100 μm. This is satisfied for ROC=556 μm. The beam size is selected for future standardized optical expanded beam connectors. Due to ellipticity of the source, the expanded beam size in the other direction is 128 μm and the beam is not fully collimated.

The most critical surface however is the one responsible for the total internal reflection of light, i.e. surface (3). Creating such surfaces in silicon that reflect light at close to 90° angle is challenging since the KOH solution etches selectively along the (111) crystalline plane, which is angled 54.7° to a standard (100) dicing face. Therefore standard wafers would

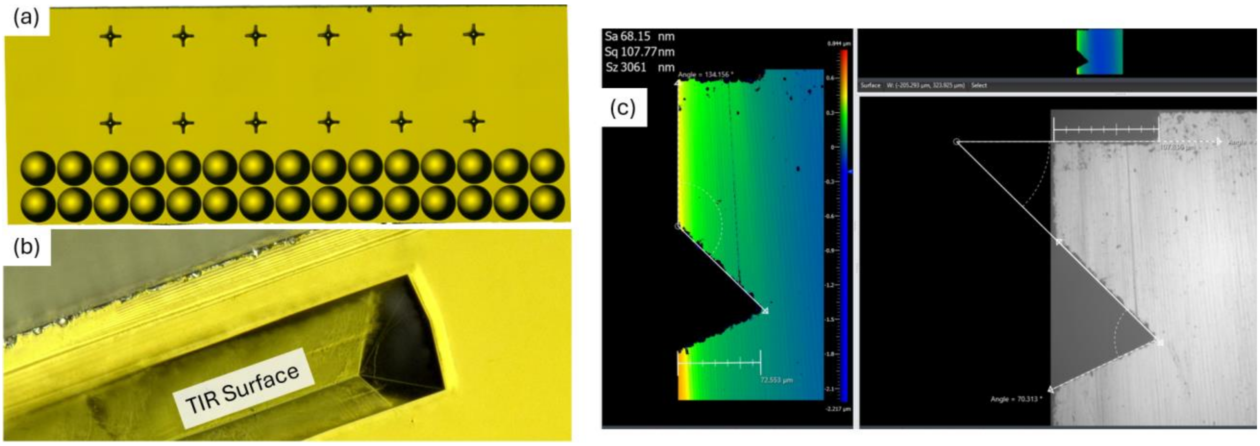

Figure 2. Photograph of the (a) top and (b) bottom surfaces of the turning mirror lens array. (c) Metrology control for the integrated prism lens: prism and vertical wall angle.

create a beam that is angled to the surface of the PIC negating the benefit of a surface-normal optical connection. For this reason, the wafer is specially miscut in order to adjust the etching plane within 1° of the 45° ideal [15][16]. Simulations suggest that such a 1° angle difference could contribute as much as 3 dB to optical losses, highlighting the importance of this fabrication step. It is also important to keep the misalignment between the bottom and top lens features within less than 1 µm (with respect to one another).

Figure 2(a) shows the photograph of the top of the turning mirror micro-lens array (MLA) fabricated by Focuslight SA. The pitch of the lenses is 250 µm. This means that every second lens is used in the array is used to couple light from the PIC as the edge coupler pitch is 500 µm. This is indicated in the photograph by the presence of alignment cross markers that in principle allow for machine-vision assistance during packaging. There are two rows of lenses depicted in the figure. Only the bottom row, the one closer to the edge, is optically active and the other row is present to maintain ROC uniformity of the array during etching. The bottom facet of the lens is shown in Figure 2(b) with the TIR surface highlighted. Extensive metrology is performed on the fabricated lens arrays, e.g. as shown in Figure 2(c). The results indicate that the prism is angled at 44.7° and the surface roughness of the TIR facet is around 50 nm. These values are satisfactory for coupling of light.

The expansion of the beam allows for the relaxation of the alignment tolerances of the connector, which itself is composed of a fiber array (FA) with a micro-lens attached to the facet. This lens is made by Focuslight from fused silica and has a

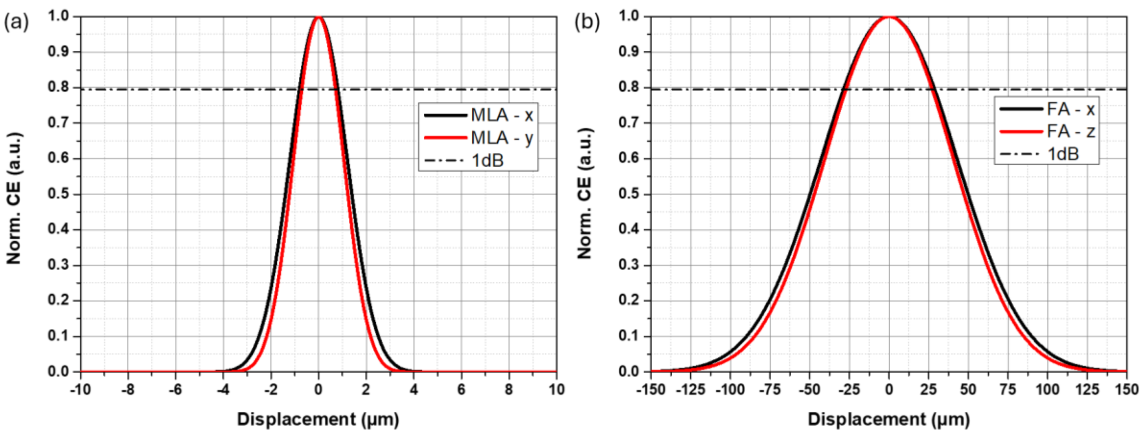

Figure 3. ZEMAX simulations of the alignment tolerances of (a) the Si lens to the PIC and (b) connectorized fiber array to the PIC assembly. CE is coupling efficiency. Horizontal line depicts 1dB threshold.

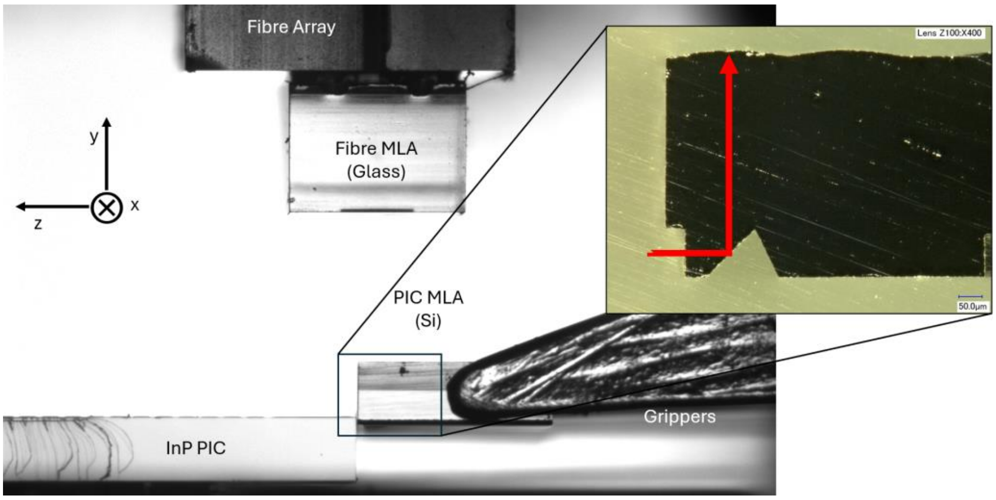

Figure 4. Side-view of the optical alignment. Inset shows a cross-section of the Si MLA. Axes describe the convention used throughout this work.

thickness of 1 mm with a ROC of 325 µm. Such a design expands a 1310 nm beam from a standard single-mode fiber to 132 µm. The mismatch between this value and the size of the PIC assembly (i.e. PIC with the turning mirror MLA aligned to the facet) beam is one of the sources of optical losses. The alignment tolerances of various components are simulated using ZEMAX and are depicted in Figure 3. Panel (a) depicts the tolerances of alignment of the Si MLA to the PIC. The 1 dB threshold is around 0.8 µm, which is tied to the small MFD of the PIC couplers. We note that these values would be similar for a butt-coupled single-mode fiber [8], albeit at a higher loss due to a larger mode mismatch. Figure 3(b) shows the impact of the beam expansion on alignment tolerances of the FA connector. They are increased by around a factor of 35 to around 28 µm with a small difference between the directions due to ellipticity of the couplers.

3. EXPERIMENTAL ALIGNMENT

The Si MLA is aligned with the PIC using nanosystec Nanoglue® alignment machine. It possesses two 6-axis alignment stages with 50 nm cardinal and < 0.005° angular precision. For the purpose of alignment an integrated low-power 1310 nm on-chip laser is powered to provide a source of light. Coupling is optimized by co-positioning the turning mirror lens held by one of the grippers and the connector held by the other. This is shown in Figure 4. The grippers holding the PIC

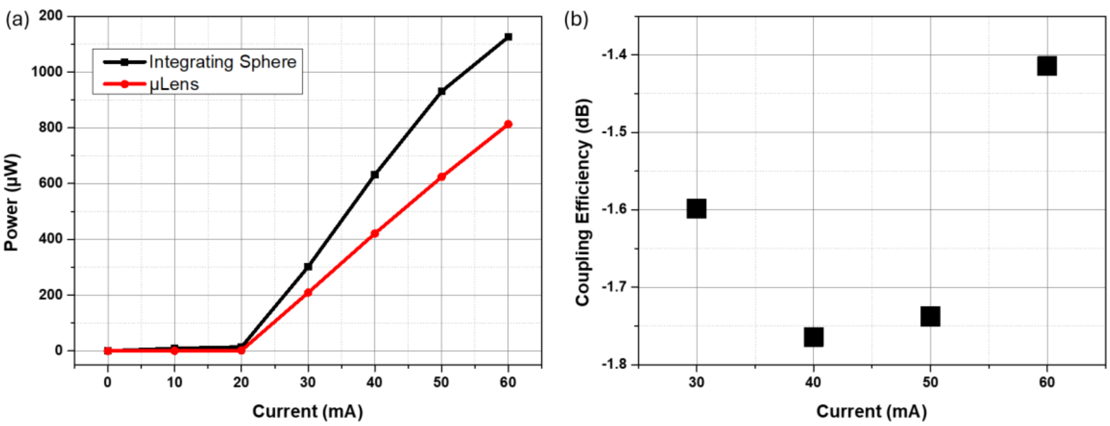

Figure 5. Determination of the coupling efficiency. (a) L-I curves comparing power coupled using an integrating sphere reference measurement and coupled using the expanded beam connection. (b) Calculated CE in dB for several values of applied current above the lasing threshold.

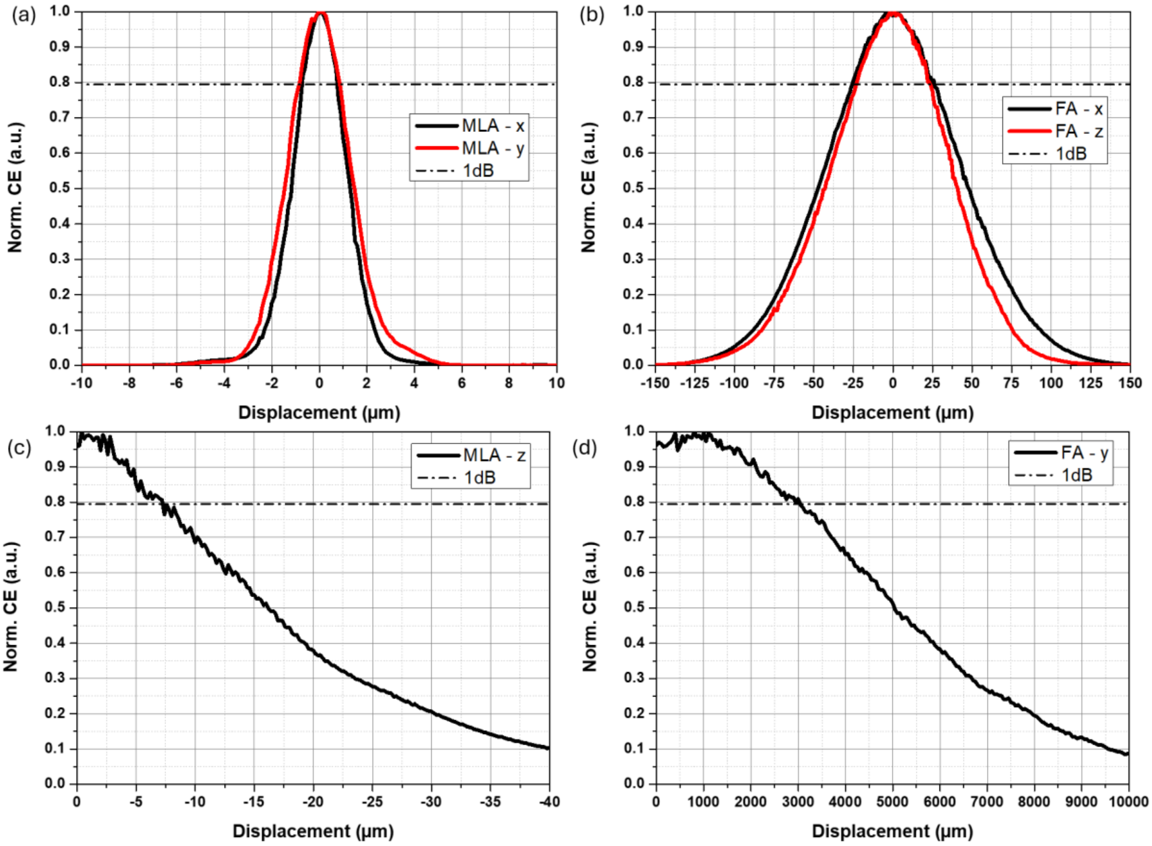

Figure 6. Measured tolerances of alignment. (a) Displacement of the Si MLA across the coupler output. (b) Displacement of connector in the plane of the PIC. (c) Axial displacement of the MLA. (d) Distance of the connector. Horizontal line depicts 1dB threshold.

MLA have to be thin and delicate enough to handle the fragile Si lens. Inset shows a cross section of the lens along with the path of light. The figure defines as well the axis convention.

In order to ascertain the coupling efficiency between the PIC and the fiber, we first perform a reference measurement where we position the output of the PIC laser against the entrance of an integrating sphere detector (Thorlabs© S144C) and measure the power for several values of applied current. The same is then repeated when the lens and connector are aligned with the PIC with the fiber output coupled to the same integrating sphere photodetector. The results are shown in Figure 5(a) with Figure 5(b) depicting difference between those curves, i.e. the coupling efficiency (CE). We observe losses in the range of 1.4-1.75 dB, which is an excellent result satisfying the benchmark of < 2 dB coupling losses set for this project. This figure can be further improved by better mode matching as well as micro-lens process control.

Figure 6 depicts a set of measured displacement curves for various axes of the Si MLA as well as the connector. The tolerance of alignment of the turning mirror lens elements is shown in panel (a). The measured alignment tolerances of 0.8 µm correspond very well with the simulated results. The connector lateral tolerances, shown in panel (b) yield similarly close results to the simulation with the measured values of 23-25 µm depending on the axis. Panel (c) shows the effect of displacement of the Si MLA along the PIC waveguide axis. In order to avoid accidental physical contact, the lens is only displaced away from the PIC from the optimal position. The 1 dB tolerance in this case is around 7 µm and is a combination of a beam walk, beam tilt and (slightly) change in beam size. Finally, the distance between the top of the PIC lens and the connector is outlined in Figure 6(d) with the optimal distance measured to be around 1 mm and with a significant 1 dB tolerance of 3 mm. Such a high tolerance to distance is a result of a very slow natural divergence of the Gaussian beam, which depends on the size of the expanded beam with larger beam sizes exhibiting smaller divergence angles [8][11].

4. CONCLUSIONS

We have presented the first 90° turning mirror silicon micro-lens scheme for coupling of light from a PIC edge coupler to the optical fiber using an expanded beam connection to relax the alignment tolerances. The achieved relaxation of tolerances is 35 times the typical alignment precision necessary to butt-couple the fiber to the PIC in a standard packaging process. This is sufficient to create a free-space optical connector that can be assembled onto a top lid of the transceiver device. With an additional design effort put into creation of a similar turning-mirror assembly on the fiber side of the connection, we can achieve a low-profile surface-mounted coupling scheme similar to a Universal Photonic Coupler from Teramount [17] or an MCP connector from SENKO [18]. The assembly of such a device can be made easier not only due to beam expansion, but also by the vertical geometry that can take advantage of precision alignment of elements using machine vision.

This is one of the components necessary for future scalable manufacturing. Another factor is to make the packaging using the presented scheme compatible with reflow as well as make it a wafer-level process where micro-lenses can be assembled not at the edge of the PIC, but on its' top utilizing e.g. micro-transfer printing [13]. With all three processes developed, packaging of photonic devices can be easily slotted into the micro-electronics packaging and assembly pipeline which allows for high scalability, as well as compatibility with legacy techniques. This will likewise contribute to decreasing the cost of photonics devices and lowering the barrier of entry for future developments.

ACKNOWLEDGEMENTS

This project has received funding from the European Union's Horizon 2020 research and innovation programme, under grant agreement number 10101673.

REFERENCES

[1] Cheng, Q., Bahadori, M., Glick, M., Rumley, S. and Bergman, K., "Recent advances in optical technologies for data centers: a review," Optica 5, 1354-1370 (2018). https://doi.org/10.1364/OPTICA.5.001354

[2] Su, P., Han, Z., Kita, F., Becla, P., Lin, H., Deckoff-Jones, S., Richardson, K., Kimerling, L. C., Hu, J. and Agarwal, A., "Monolithic on-chip mid-IR methane gas sensor with waveguide-integrated detector," Appl. Phys. Lett. 114, 051103 (2019). https://doi.org/10.1063/1.5053599

[3] Kazanskiy, N. L., Khonina, S. N., Butt, M. A., Kaźmierczak, A. and Piramidowicz, R., "State-of-the-Art Optical Devices for Biomedical Sensing Applications—A Review," Electronics 10(8), 973 (2021). https://doi.org/10.3390/electronics10080973

[4] Tan, M., Xu, J., Liu, S. *et al.* "Co-packaged optics (CPO): status, challenges, and solutions," Front. Optoelectron. 16, 1 (2023). https://doi.org/10.1007/s12200-022-00055-y

[5] Maniotis, P. and Kuchta, D. M., "Exploring the benefits of using co-packaged optics in data center and AI supercomputer networks: a simulation-based analysis [Invited]," J. Opt. Commun. Netw. 16, A143-A156 (2024). https://doi.org/10.1364/JOCN.501427

[6] Carroll, L., Lee, J. S., Scarcella, C., Gradkowski, K., Duperron, M., Lu, H., Zhao, Y., Eason, C., Morrissey, P. M., Rensing, M., Collins, S., Hwang, H. Y. and O'Brien, P., "Photonic packaging: transforming silicon photonic integrated circuits into photonic devices," Appl. Sci. 6(12), 426 (2016). https://doi.org/10.3390/app6120426

[7] Zhang, J., Chen, P. and Wang, K., "Design and Optimization of Edge Couplers for High-Efficiency Fiber-to-PIC Coupling," Appl. Sci. 10(4), 1538–1546 (2020). https://doi.org/10.3390/app10041538

[8] Gradkowski, K., "Tolerances of the alignment of fibers to photonic integrated circuits," Appl. Opt. 63, 8407-8412 (2024). https://doi.org/10.1364/AO.540682

[9] Du, Y., Wang, F., Hong, Z., Shi, Y., Chen, X. and Zheng, X, "Detachable interface toward a low-loss reflow-compatible fiber coupling for co-packaged optics (CPO)," Opt. Express 31, 1318-1329 (2023). https://doi.org/10.1364/OE.480418

[10] Scarcella, C. Gradkowski, K., Carroll, L., Lee, J. S., Duperrron, M., Fowler, D. and O'Brien, P., "Pluggable Single-Mode Fiber-Array-to-PIC Coupling Using Micro-Lenses," IEEE Photonics Techn. Lett. 29(22), 1943-1946 (2017). https://doi.org/10.1109/LPT.2017.2757082
[11] Gradkowski, K., Stegall, D., Mackey, D., Naughton, A., Smith, T. and O'Brien P., "Demonstration of a Single-Mode Expanded-Beam Connectorized Module for Photonic Integrated Circuits," J. Lightwave Technol. 41, 3470-3478 (2023). https://doi.org/10.1109/JLT.2023.3239138
[12] Gradkowski, K., Morrissey, P. M. and O'Brien P., "Packaging of micro-lens arrays to photonic integrated circuits using beam shape evaluation," J. Phys. Photonics 6, 035022 (2024). https://doi.org/10.1088/2515-7647/ad5bd2
[13] Wakeel, S., Morrissey, P. M., Genc, M., Ramaswamy, P., Bernson, R., Gradkowski, K., Corbett, B. and O'Brien P., "Micro-transfer printing of thick optical components using a tether-free UV-curable approach," J. Opt. Microsyst. 4(1), 011003 (2024). https://doi.org/10.1117/1.JOM.4.1.011003
[14] Marchetti, R., Lacava, C., Carroll, L., Gradkowski, K. and Minzioni P., "Coupling strategies for silicon photonics integrated chips [Invited]," Photon. Res. 7, 201 (2019). https://doi.org/10.1364/PRJ.7.000201
[15] Zheng, X., Cunningham, J. E., Shubin, I., Simons, J., Asghari, M., Feng, D., Lei, H., Zheng, D., Liang, H. Kung, C., Luff, J., Sze, T., Cohen, D. and Krishnamoorthy, A. V., "Optical proximity communication using reflective mirrors," Opt. Express 16, 15052-15058 (2008). https://doi.org/10.1364/OE.16.015052
[16] Rola, K.P., "Anisotropic etching of silicon in KOH + Triton X-100 for 45° micromirror applications," Microsyst Technol 23, 1463–1473 (2017). https://doi.org/10.1007/s00542-016-3103-0
[17] Teramount Ltd.: https://teramount.com/products/
[18] SENKO MPC Connector: https://www.senko.com/wp-content/uploads/2023/02/Placard-FA-vs-MPC.pdf